AIAA Journal
Vol. 59, No. 11, November 2021

Technical Notes

Lighthill Stress Flux Model for Ffowcs Williams–Hawkings Integrals in Frequency Domain

Zhiteng Zhou,* Hongping Wang,† Shizhao Wang,‡ and Guowei He§
State Key Laboratory of Nonlinear Mechanics, Chinese Academy of Sciences, 100190 Beijing, People's Republic of China

https://doi.org/10.2514/1.J060070

Nomenclature

c_o	=	speed of sound
G_{2D}	=	two-dimensional Green's function
G_{3D}	=	three-dimensional Green's function
k	=	wave number
M	=	freestream Mach number
P_{ij}	=	compressive stress tensor
p_o	=	pressure in the background
p'	=	perturbation of pressure
T_{ij}	=	Lighthill stress tensor
U_i	=	freestream velocity
U_p	=	phase velocity flows
u_i	=	Cartesian velocity components
x_i	=	Cartesian observer coordinates
y_i	=	Cartesian source coordinates
ρ'	=	perturbation of density
ω	=	frequency

I. Introduction

THE objective of this short Note is to derive a model to diminish the spurious sound caused by vortical flows crossing the permeable Ffowcs Williams and Hawkings (FW-H) integral surfaces. The FW-H integrals are the solutions of the FW-H equation, which extends Lighthill's acoustic analogy method to flows with arbitrary moving boundaries. The FW-H integrals consist of surface integrals associated with monopole and dipole sources on solid/permeable boundaries and a volume integral associated with quadrupole sources external to the boundaries [1]. The volume integral is usually neglected in computing the far-field sound with the assumption that the sound is dominated by the surface integrals associated with monopole and dipole sources because the computation of the volume integral associated with the quadrupole sources is prohibitively expensive for flows of practical interest. However, recent research has shown that neglecting the volume integrals may cause spurious contributions to the far-field sound even for flows at relatively low Mach numbers [2–4]. This is because the vortical flows crossing the integral surfaces generate spurious boundary noise that contaminates the acoustic field [5–7].

The spurious boundary noise has been eliminated by reformulating the volume integral associated with the quadrupole sources to an additional surface integral in the works of Wang et al. [7] and Ikeda et al. [2] for Curle's equation and the FW-H equation, respectively. The methodology is based on the assumption that the Lighthill stress fluxes near the exit boundaries are convected by frozen flow. Therefore, the quadrupole sources external to the boundaries can be approximated by a flux term evaluated on the boundaries. The correct computation of the Lighthill stress flux or the determination of the convective velocity is crucial to eliminate spurious sound.

Wang et al. [7] determined the convective velocity of the frozen flow by scaling the freestream velocity. The spurious sound was successfully eliminated for a class of problems in which vortices leave the integral surfaces at a nearly constant velocity. Ikeda et al. [2] improved the computation of Lighthill stress flux to account for the nonuniform convection for locally subsonic flows. Nitzkorski and Mahesh [8] proposed a dynamic end cap technique where the quadrupole source is correlated over multiple planes to determine the convective velocity to allow for a small but customizable volume computation. Rahier et al. [9] further improved the computation of flux by accounting for the Doppler amplification effects associated with the flow velocity and surface moving velocity. The time-domain formulations for the additional surface integral have successfully predicted the contribution of the volumetric quadrupole integral with a fixed or moving control surface. However, the extension of the time-domain formulations to the frequency domain has not been clearly addressed until recently [10].

Lockard and Casper [11] proposed a frequency-domain formulation that approximated the volumetric quadrupole integral by a series of surface integrals. The series of surface integrals was derived by using the integration by parts repeatedly, which involves computing the high-order derivatives of Green's function. The model was found to work reasonably well in several test cases. However, the high-order derivatives of Green's function are quite complicated and nontrivial to calculate [11]. Moreover, the convergence of the series depends on the Mach number and the observer positions. The series is divergent in computing the sound generated by a two-dimensional (2-D) convecting vortex for observers upstream when the Mach number is 0.6. Ikeda et al. [10] fixed this problem by deriving a frequency-domain formulation via a Fourier transform applied to the time-domain formulation. In the present work, we propose an alternative method to fix the divergence problem.

The proposed method is based on a Lighthill stress flux model to evaluate the additional surface integral that approximates the volumetric quadrupole integral. The model is robust to compute the far-field sound generated by subsonic flows at different Mach numbers. We also try to explore the physics that causes the divergence of the series reported in the work of Lockard and Casper [11]. Furthermore, we simplify the computation of the high-order derivatives of Green's function based on far-field approximations and provide a single surface integral to avoid computing the series of surface integrals, resulting in an efficient way to account for the contribution of the vortical flows outside the boundaries. We will briefly introduce the

Received 13 August 2020; revision received 13 June 2021; accepted for publication 21 June 2021; published online 28 July 2021.

*Ph.D. Candidate, Institute of Mechanics; also School of Engineering Sciences, University of Chinese Academy of Sciences, 100049 Beijing, People's Republic of China.

†Postdoctoral Research Scientist, Institute of Mechanics; also School of Engineering Sciences University of Chinese Academy of Sciences, 100049 Beijing, People's Republic of China.

‡Professor, Institute of Mechanics; also School of Engineering Sciences, University of Chinese Academy of Sciences, 100049 Beijing, People's Republic of China; wangsz@lnm.imech.ac.cn (Corresponding Author).

§Professor, Institute of Mechanics; also School of Engineering Sciences, University of Chinese Academy of Sciences, 100049 Beijing, People's Republic of China.

acoustic equations in Sec. II, discuss the proposed Lighthill stress flux model that diminishes the spurious sound in Sec. III, validate the proposed method in Sec. IV, and draw conclusions in Sec. V.

II. Acoustic Equations

We compute the sound generated by sources in a uniformly moving media as in the works of Lockard and Casper [11] and Wang et al. [7]. The FW-H equation in differential form can be written as

$$\left(\frac{\partial^2}{\partial t^2} + U_i U_j \frac{\partial^2}{\partial x_i \partial x_j} + 2U_i \frac{\partial^2}{\partial x_i \partial t} - c_o^2 \frac{\partial^2}{\partial x_i \partial x_i}\right)(H(f)\rho') = \frac{\partial^2}{\partial x_i \partial x_j}(T_{ij}H(f)) - \frac{\partial}{\partial x_i}(F_i \delta(f)) + \frac{\partial}{\partial t}(Q\delta(f)) \quad (1)$$

where

$$\begin{aligned} T_{ij} &= \rho u_i u_j + P_{ij} - c_o^2 \rho' \delta_{ij}, \\ F_i &= (P_{ij} + \rho(u_i - U_i)(u_j + U_j) + \rho_o U_i U_j) n_j, \\ Q &= (\rho(u_i + U_i) - \rho_o U_i) n_i \end{aligned} \quad (2)$$

ρ_o, c_o, and p_o are the density, speed of sound, and pressure of the ambient flow, respectively; and $\rho' = \rho - \rho_o$ and $p' = p - p_o$ are perturbations of the density and pressure, respectively. A level set function $f = 0$ is used to denote the boundaries outside of which the solution is desired (hereinafter referred to as the FW-H surface). Note that n_i is the unit normal vector of the boundaries. The FW-H surface is fixed in uniform flow as in the work of Lockard and Casper [11]. $H(f)$ is the Heaviside function, which is equal to one for $f > 0$ and zero for $f < 0$. T_{ij} is the Lighthill stress tensor, $P_{ij} = (p - p_0)\delta_{ij} - \tau_{ij}$ is the compressive stress tensor, and τ_{ij} is the viscous stress tensor. According to the work of Lockard and Casper [11], the viscous stress tensor in the Lighthill stress tensor is neglected. The solution to Eq. (1) in the frequency domain can be given by the integrals as follows (hereinafter referred to as FW-H integrals) [12]:

$$H(f) c_o^2 \rho'(\boldsymbol{x}, \omega) = I_T + I_L + I_Q \quad (3)$$

where I_T, I_L, and I_Q are contributions of the thickness, loading, and quadrupole terms, respectively,

$$\begin{aligned} I_T(\boldsymbol{x}, \omega) &= -\int_{f=0} \mathrm{i}\omega Q(\boldsymbol{y}, \omega) G(\boldsymbol{x}; \boldsymbol{y})\, \mathrm{d}S, \\ I_L(\boldsymbol{x}, \omega) &= -\int_{f=0} F_i(\boldsymbol{y}, \omega) \frac{\partial G(\boldsymbol{x}; \boldsymbol{y})}{\partial x_i}\, \mathrm{d}S \end{aligned} \quad (4)$$

$$I_Q(\boldsymbol{x}, \omega) = -\int_{f>0} T_{ij}(\boldsymbol{y}, \omega) \frac{\partial^2 G(\boldsymbol{x}; \boldsymbol{y})}{\partial y_i \partial y_j}\, \mathrm{d}V \quad (5)$$

where $\boldsymbol{x}$ and $\boldsymbol{y}$ are the observer position and source position, respectively. G is Green's function of the convection wave equation corresponding to Eq. (1) at $M < 1$. Note that $\rho'(\boldsymbol{x}, \omega)$, $Q(\boldsymbol{y}, \omega)$, $F_i(\boldsymbol{y}, \omega)$, and $T_{ij}(\boldsymbol{y}, \omega)$ are the Fourier transforms of time-domain variables ρ', Q, F_i, and T_{ij}, respectively.

III. Corrections for the Quadrupole Term

The direct computation of the volume integrals of the quadrupole term in the form of Eq. (5) is prohibitively expensive. Therefore, we propose a model to compute the contributions of the volume integral. In accordance with the setups of Lockard and Casper [11] and Wang et al. [7], we take the mean flow that carries the frozen vortices along the y_1 direction. By repeatedly using the integration by parts, we reformulate Eq. (5) as follows:

$$\begin{aligned} I_Q(\boldsymbol{x}; \omega) &= -\int_{f>0} T_{ij}(\boldsymbol{y}, \omega) \frac{\partial^2 G(\boldsymbol{x}; \boldsymbol{y})}{\partial y_i \partial y_j}\, \mathrm{d}V \\ &= -\int_{f>0} \left(\frac{\partial}{\partial y_1} \left(T_{ij}(\boldsymbol{y}, \omega) I^1 \left(\frac{\partial^2 G(\boldsymbol{x}; \boldsymbol{y})}{\partial y_i \partial y_j} \right) \right) \right. \\ &\quad - \frac{\partial}{\partial y_1} \left(\frac{\partial T_{ij}(\boldsymbol{y}, \omega)}{\partial y_1} I^2 \left(\frac{\partial^2 G(\boldsymbol{x}; \boldsymbol{y})}{\partial y_i \partial y_j} \right) \right) + \cdots \\ &\quad + (-1)^n \frac{\partial}{\partial y_1} \left(\frac{\partial^n T_{ij}(\boldsymbol{y}, \omega)}{\partial y_1^n} I^{n+1} \left(\frac{\partial^2 G(\boldsymbol{x}; \boldsymbol{y})}{\partial y_i \partial y_j} \right) \right) \\ &\quad \left. + (-1)^{n+1} \left(\frac{\partial^{n+1} T_{ij}(\boldsymbol{y}, \omega)}{\partial y_1^{n+1}} I^{n+1} \left(\frac{\partial^2 G(\boldsymbol{x}; \boldsymbol{y})}{\partial y_i \partial y_j} \right) \right) \right) \mathrm{d}V \end{aligned} \quad (6)$$

where

$$I^n \left(\frac{\partial^2 G(\boldsymbol{x}; \boldsymbol{y})}{\partial y_i \partial y_j} \right) \stackrel{\text{def}}{=} \int_\infty^{y_1} \left(\int_\infty^{\xi_n} \left(\int_\infty^{\xi_{n-1}} \left(\cdots \int_\infty^{\xi_3} \left(\int_\infty^{\xi_2} \frac{\partial^2 G(\boldsymbol{x}; \xi_1, y_2)}{\partial y_i \partial y_j}\, \mathrm{d}\xi_1 \right) \times \mathrm{d}\xi_2 \cdots \right) \mathrm{d}\xi_{n-2} \right) \mathrm{d}\xi_{n-1} \right) \mathrm{d}\xi_n \quad (7)$$

is the multiple integral of

$$\frac{\partial^2 G(\boldsymbol{x}; \boldsymbol{y})}{\partial y_i \partial y_j}$$

For the ith integral ($i < n$) from the inner of the integral of Eq. (7), the independent variable is ξ_i and the upper limit of the integral is ξ_{i+1}. When $i = n$, the independent variable is ξ_n and the upper limit of the integral is y_1.

By integrating the right-hand-side terms of Eq. (6) along the y_1 direction, we obtain the integral on the FW-H surface as follows:

$$\begin{aligned} I_Q(\boldsymbol{x}; \omega) &= -\int_{f>0} (-1)^{n+1} \left(\frac{\partial^{n+1} T_{ij}(\boldsymbol{y}, \omega)}{\partial y_1^{n+1}} I^{n+1} \left(\frac{\partial^2 G(\boldsymbol{x}; \boldsymbol{y})}{\partial y_i \partial y_j} \right) \right) \mathrm{d}V \\ &\quad + \sum_{l=0}^{n} \int_{f=0} (-1)^l \left(\frac{\partial^l T_{ij}(\boldsymbol{y}, \omega)}{\partial y_1^l} I^{l+1} \left(\frac{\partial^2 G(\boldsymbol{x}; \boldsymbol{y})}{\partial y_i \partial y_j} \right) \right) \mathrm{d}S \end{aligned} \quad (8)$$

Green's functions for the convective wave equations in 2-D and three dimensions (3-D) are [11]

$$G_{2D}(\boldsymbol{x}; \boldsymbol{y}) = \frac{\mathrm{i}}{4\beta} \exp^{(\mathrm{i}Mk(x_1 - y_1)/\beta^2)} H_0^{(2)} \left(\frac{k}{\beta^2} R \right) \quad (9)$$

$$G_{3D}(\boldsymbol{x}; \boldsymbol{y}) = \frac{-1}{4\pi d} \exp^{\varphi_{3D}(\boldsymbol{x}; \boldsymbol{y})} \quad (10)$$

where M is the Mach number. $H_0^{(2)}$ is the zero-order Hankel function of the second kind:

$$\begin{aligned} \beta &= \sqrt{1 - M^2}, \qquad k = \omega / c_o, \\ R &= \sqrt{(x_1 - y_1)^2 + \beta^2 (x_2 - y_2)^2}, \\ d &= \sqrt{(x_1 - y_1)^2 + \beta^2 (x_2 - y_2)^2 + \beta^2 (x_3 - y_3)^2}, \\ \varphi_{3D} &= -\mathrm{i}k(d - M(x_1 - y_1)) / \beta^2 \end{aligned} \quad (11)$$

In the far field, by employing the asymptotic form of the Hankel function [13], Eq. (9) reduces to

$$\begin{aligned} G_{2D}(\boldsymbol{x}; \boldsymbol{y}) &\approx \frac{\mathrm{i}}{4\beta} \left(\frac{2\beta^2}{\pi k R} \right)^{1/2} \exp^{\varphi_{2D}(\boldsymbol{x}; \boldsymbol{y})}, \\ \varphi_{2D}(\boldsymbol{x}; \boldsymbol{y}) &= \mathrm{i} \left(Mk(x_1 - y_1)/\beta^2 + \frac{\pi}{4} - \frac{k}{\beta^2} R \right) \end{aligned} \quad (12)$$

The far-field asymptotic form of the derivatives of Green's functions in 2-D and 3-D can be approximated as follows [14]:

$$\frac{\partial^l}{\partial y_1^l}\left(\frac{\partial^2 G_{2D}(\boldsymbol{x};\boldsymbol{y})}{\partial y_i \partial y_j}\right) \approx \left(\frac{\partial \varphi(\boldsymbol{x};\boldsymbol{y})}{\partial y_1}\right)_{2D}^l \frac{\partial^2 G_{2D}(\boldsymbol{x};\boldsymbol{y})}{\partial y_i \partial y_j} \tag{13a}$$

$$I^l\left(\frac{\partial^2 G_{2D}(\boldsymbol{x};\boldsymbol{y})}{\partial y_i \partial y_j}\right) \approx \left(\frac{\partial \varphi(\boldsymbol{x};\boldsymbol{y})}{\partial y_1}\right)_{2D}^{-l} \frac{\partial^2 G_{2D}(\boldsymbol{x};\boldsymbol{y})}{\partial y_i \partial y_j} \tag{13b}$$

$$\frac{\partial^l}{\partial y_1^l}\left(\frac{\partial^2 G_{3D}(\boldsymbol{x};\boldsymbol{y})}{\partial y_i \partial y_j}\right) \approx \left(\frac{\partial \varphi(\boldsymbol{x};\boldsymbol{y})}{\partial y_1}\right)_{3D}^l \frac{\partial^2 G_{3D}(\boldsymbol{x};\boldsymbol{y})}{\partial y_i \partial y_j} \tag{14a}$$

$$I^l\left(\frac{\partial^2 G_{3D}(\boldsymbol{x};\boldsymbol{y})}{\partial y_i \partial y_j}\right) \approx \left(\frac{\partial \varphi(\boldsymbol{x};\boldsymbol{y})}{\partial y_1}\right)_{3D}^{-l} \frac{\partial^2 G_{3D}(\boldsymbol{x};\boldsymbol{y})}{\partial y_i \partial y_j} \tag{14b}$$

According to Eqs. (13) and (14), Eq. (8) can be approximately expressed as follows to avoid the complicated computation of the derivatives and integrals of Green's function:

$$\begin{aligned} I_Q(\boldsymbol{x};\omega) &= -\int_{f>0} (-1)^{n+1}\left(\frac{\partial^{n+1} T_{ij}(\boldsymbol{y},\omega)}{\partial y_1^{n+1}}\left(\frac{\partial \varphi(\boldsymbol{x};\boldsymbol{y})}{\partial y_1}\right)^{-n-1}\frac{\partial^2 G(\boldsymbol{x};\boldsymbol{y})}{\partial y_i \partial y_j}\right)\mathrm{d}V \\ &+\sum_{l=0}^{n}\int_{f=0}(-1)^l\left(\frac{\partial^l T_{ij}(\boldsymbol{y},\omega)}{\partial y_1^l}\left(\frac{\partial \varphi(\boldsymbol{x};\boldsymbol{y})}{\partial y_1}\right)^{-l-1}\frac{\partial^2 G(\boldsymbol{x};\boldsymbol{y})}{\partial y_i \partial y_j}\right)\mathrm{d}S \end{aligned} \tag{15}$$

Equation (15) consists of a volume integral and a series of surface integrals. The integrands in Eq. (15) are different from the model proposed by Lockard and Casper [11] because different ways of integration by parts are used. Equation (15) gives an alternative series of surface integrals to approximate I_Q by dropping the volume integral. We will show later that the convergence of the series depends on the convective velocity and the phase velocity of a perturbation propagating in the convective flow. Note that Eq. (15) is derived without the assumption of frozen flows crossing the integral surfaces. In this sense, the volume integral of the quadrupole term I_Q in Eq. (5) can be approximately evaluated by surface integrals on the boundaries without referring to the frozen flows assumption. However, the series of the surface integrals in Eq. (15) involves the high-order derivatives of the Lighthill stress tensor, which is difficult to compute or measure. We use the frozen vortices assumption as follows to avoid the computation of high-order derivatives of the Lighthill stress tensor:

$$\frac{\partial T_{ij}(\boldsymbol{y})}{\partial t} + U_1 \frac{\partial T_{ij}(\boldsymbol{y})}{\partial y_1} = 0 \tag{16}$$

where U_1 is the uniform freestream velocity along the y_1 direction. Using the Fourier transform of Eq. (16), the spatial derivatives of the Lighthill stress tensor can be represented by the time derivatives in the frequency domain; and Eq. (15) reduces to

$$\begin{aligned} I_Q(\boldsymbol{x};\omega) &= -\int_{f>0}\left(\frac{\mathrm{i}\omega}{U_1}\right)^{n+1} T_{ij}(\boldsymbol{y},\omega)\left(\frac{\partial \varphi(\boldsymbol{x};\boldsymbol{y})}{\partial y_1}\right)^{-n-1}\frac{\partial^2 G(\boldsymbol{x};\boldsymbol{y})}{\partial y_i \partial y_j}\mathrm{d}V \\ &+\sum_{l=0}^{n}\int_{f=0}\left(\frac{\mathrm{i}\omega}{U_1}\right)^{l} T_{ij}(\boldsymbol{y},\omega)\left(\frac{\partial \varphi(\boldsymbol{x};\boldsymbol{y})}{\partial y_1}\right)^{-l-1}\frac{\partial^2 G(\boldsymbol{x};\boldsymbol{y})}{\partial y_i \partial y_j}\mathrm{d}S \end{aligned} \tag{17}$$

When

$$\left|\frac{\mathrm{i}\omega}{U_1}\left(\frac{\partial \varphi(\boldsymbol{x};\boldsymbol{y})}{\partial y_1}\right)^{-1}\right| < 1$$

and $n \to \infty$, the volume integral term on the right-hand side of Eq. (17) vanishes, and the series of surface integrals reduces to the model proposed by this work as follows:

$$I_Q(\boldsymbol{x};\omega) = \int_{f=0} \frac{\mathrm{i}U_1}{\mathrm{i}U_1(\partial\varphi/\partial y_1)+\omega} T_{ij}(\boldsymbol{y},\omega)\frac{\partial^2 G(\boldsymbol{x};\boldsymbol{y})}{\partial y_i \partial y_j}\,\mathrm{d}S \tag{18}$$

The model proposed by Lockard and Casper [11] for the quadrupole term is

$$\begin{aligned} I_Q(\boldsymbol{x};\omega) = &-\int_{f>0}\left(\frac{-\mathrm{i}U_1}{\omega}\right)^n T_{ij}(\boldsymbol{y},\omega)\frac{\partial^n}{\partial y_1^n}\left(\frac{\partial^2 G(\boldsymbol{x};\boldsymbol{y})}{\partial y_i \partial y_j}\right)\mathrm{d}V \\ &-\sum_{l=1}^{n}\int_{f=0}\left(\frac{-\mathrm{i}U_1}{\omega}\right)^l T_{ij}(\boldsymbol{y},\omega)\frac{\partial^{l-1}}{\partial y_1^{l-1}}\left(\frac{\partial^2 G(\boldsymbol{x};\boldsymbol{y})}{\partial y_i \partial y_j}\right)\mathrm{d}S \end{aligned} \tag{19}$$

To approximate the high-order derivative of Green's function by using Eq. (13a) or Eq. (14a), Eq. (19) yields

$$\begin{aligned} I_Q(\boldsymbol{x};\omega) = &-\int_{f>0}\left(\frac{U_1}{\mathrm{i}\omega}\right)^n T_{ij}(\boldsymbol{y},\omega)\left(\frac{\partial \varphi(\boldsymbol{x};\boldsymbol{y})}{\partial y_1}\right)^n\frac{\partial^2 G(\boldsymbol{x};\boldsymbol{y})}{\partial y_i \partial y_j}\mathrm{d}V \\ &-\sum_{l=1}^{n}\int_{f=0}\left(\frac{U_1}{\mathrm{i}\omega}\right)^l T_{ij}(\boldsymbol{y},\omega)\left(\frac{\partial \varphi(\boldsymbol{x};\boldsymbol{y})}{\partial y_1}\right)^{l-1}\frac{\partial^2 G(\boldsymbol{x};\boldsymbol{y})}{\partial y_i \partial y_j}\mathrm{d}S \end{aligned} \tag{20}$$

When

$$\left|\frac{U_1}{\mathrm{i}\omega}\frac{\partial \varphi(\boldsymbol{x};\boldsymbol{y})}{\partial y_1}\right| < 1$$

and $n \to \infty$, the volume integral term on the right-hand side of Eq. (20) vanishes and the series of surface integrals reduces exactly to Eq. (18).

It is noted that

$$\frac{\mathrm{i}\omega}{U_1}\left(\frac{\partial \varphi(\boldsymbol{x};\boldsymbol{y})}{\partial y_1}\right)^{-1} \neq +1$$

for subsonic flows [14], and therefore the denominator in Eq. (18) does not vanish. Equation (18) is still valid when

$$\frac{\mathrm{i}\omega}{U_1}\left(\frac{\partial \varphi(\boldsymbol{x};\boldsymbol{y})}{\partial y_1}\right)^{-1} = -1$$

because the volume integral term on the right-hand side of Eq. (17) or Eq. (20) can be combined with the left-hand-side term [14], and the alternating series can be reformulated into Eq. (18).

Compared with the previous model in Eq. (19), the proposed model [Eq. (18)] has only one single surface integral instead of a series of surface integrals. The proposed model [Eq. (18)] only requires the computation of the second-order derivatives of the Green's function, whereas the previous model [Eq. (19)] requires the computation of high-order derivatives of the Green's function. As pointed out by Lockard and Casper [11], the computations of high-order derivatives are quite complicated and nontrivial. Ikeda et al. [10] gave the frequency-domain formulation for three-dimensional flows and treated the two-dimensional flows as three-dimensional flows with the identical source distributions along the spanwise direction. The present work directly gives the formulation for both two-dimensional and three-dimensional flows. Moreover, Eq. (18) is valid for flows with both

$$\left|\frac{\mathrm{i}\omega}{U_1}\left(\frac{\partial \varphi(\boldsymbol{x};\boldsymbol{y})}{\partial y_1}\right)^{-1}\right| < 1$$

and

$$\left|\frac{\mathrm{i}\omega}{U_1}\left(\frac{\partial \varphi(\boldsymbol{x};\boldsymbol{y})}{\partial y_1}\right)^{-1}\right| > 1$$

Note that

$$U_p \stackrel{\text{def}}{=} \mathrm{i}\omega\left(\frac{\partial\varphi(\boldsymbol{x};\boldsymbol{y})}{\partial y_1}\right)^{-1}$$

is the phase velocity of a perturbation propagating in the convective flow. The series of surface integrals in Eq. (19) only converges when the convective velocity U_1 is slower than U_p. For flows with a relatively large Mach number based on the uniform freestream velocity and the ambient speed of sound, the convective velocity might be larger than U_p at some observer positions. This is the reason that the series of surface integrals in Eq. (19) becomes divergent when predicting the sound at an observer upstream of the 2-D convecting vortex with a Mach number of $M = U_1/c_0 = 0.6$, as we will discuss in the next section. Equation (18) circumvents this divergence problem by using different ways of integration by parts.

It is worth mentioning that both Eq. (18) and the discussion of the convergence conditions are consistent with the frequency-domain formulation derived via the Fourier transform of the time-domain formulation [10]. We derived the additional surface integral by using integration by parts and the far-field asymptotic Green's functions. The proposed model provides an alternative perspective to investigate the physics of the divergence problem reported in the previous work, and the formulation has the capability of efficiently computing the far-field sound pressure in 2-D problems. Despite that different approaches and mathematical formulations are employed, the consistence of the results with the work of Ikeda et al. [10] provides another support to the validity of the model proposed by the present work.

IV. Validation

It has been reported that the series of surface integrals in Eq. (19) becomes divergent when predicting the sound generated by a 2-D convecting vortex at $M = 0.6$ as the observer moves from downstream to upstream [11]. First, we show the superiority of the proposed model in handling the case ($M = 0.6$) where the previous model [Eq. (19)] is divergent. Then, we show that the proposed model can identify the causes of the divergence reported in the previous work [11]. Finally, we discuss the advantages of the proposed model by investigating the convergence diagram.

The pressure and velocity of the 2-D convecting vortex are given in Ref. [11] as the following:

$$p = \frac{1}{\gamma}(1 - a_2\exp(1 - r^2))^{\gamma/\gamma-1}, \quad \rho = \left(\frac{p}{p_o}\right)^{1/\gamma},$$
$$u = U_1 - a_0 a_1 y_2 \exp((1 - r^2)/2),$$
$$v = a_0 a_1 (y_1 - Mt)\exp((1 - r^2)/2) \tag{21}$$

where

$$a_0 = 1, \qquad a_1 = 1/(2\pi), \qquad a_2 = (\gamma - 1)a_0^2 a_1^2/2,$$
$$r^2 = (y_1 - Mt)^2 + y_2^2 \tag{22}$$

where $\gamma = 1.4$ is the specific heat ratio of air. Note that p_o is the pressure in the background flow. All the variables are normalized according to the work of Lockard and Casper [11]. The reference velocity, length, density, time, and pressure are the ambient speed of sound c_o, the length L referred to the work of Casper and Lockard [11], the density of ambient fluid ρ_o, L/c_o, and $\rho_o c_o^2$, respectively. The upstream and downstream observer positions are at a distance of $100L$ from the initial center of the vortex. The vortex moves along the y_1 direction at a Mach number of $M = U_1/c_o$ and remains frozen during the motion. The pressure gradually approaches the constant $1/\gamma$ in the far field, which indicates that the sound at the far field is zero. A permeable square with each side of length 10 is used as the FW-H integral surface.

When the quadrupole term in Eq. (5) is neglected, the FW-H integrals [Eq. (4)] on the permeable square surface will result in significant spurious sound, as shown by the solid lines with open circles labeled as FWH2D in Fig. 1, where observers are at a radius of 100. The negative of the quadrupole term (I_Q in Fig. 1) computed by using the proposed model [Eq. (18)] agrees well with the summary of the monopole and dipole terms, which means that the proposed model can effectively diminish the spurious sound. The proposed method is valid in both the downstream and upstream directions. The series of surface integrals with $n = 1$ and $n = 2$ in Eq. (19) gives an approximation to the quadrupole terms at the downstream observer position but diverges at the upstream observer position. The divergence of the series at the upstream observer positions can be investigated by referring to Eq. (20), which is the approximation of Eq. (19) with far-field asymptotics according to Ref. [14]. The phase velocity of a perturbation propagating in the convective flows can be approximated by

$$U_p \equiv \mathrm{i}\omega\left(\frac{\partial\varphi(\boldsymbol{x};\boldsymbol{y})}{\partial y_1}\right)^{-1} = \frac{c_o(1 - M^2)}{-M + (x_1 - y_1/R)} \tag{23}$$

At the far-field upstream observer positions, $x_1 - y_1/R \approx -1$; and Eq. (23) reduces to

$$U_p \approx \frac{c_o(1 - M^2)}{-M - 1} = c_o(M - 1) \tag{24}$$

The scale factor in the series of surface integrals in Eq. (20) reduces to

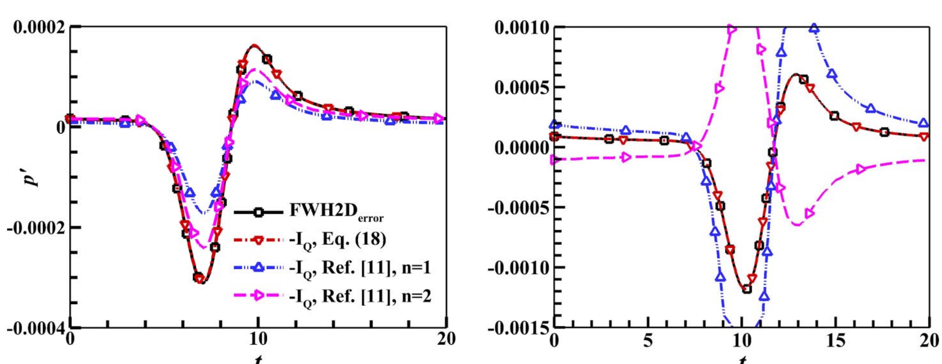

Fig. 1 Comparison of the quadrupole correction I_Q to the errors produced by FWH2D ($I_L + I_T$) at $M = 0.6$ at a) downstream observer ($\theta = 0$) and b) upstream observer ($\theta = \pi$).

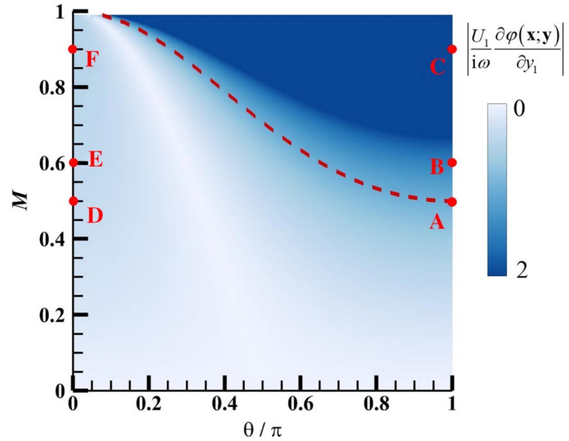

Fig. 2 Convergence diagram for flows at different Mach numbers and observers at different directivities. Markers A ($M = 0.5$, $\theta = \pi$), B ($M = 0.6$, $\theta = \pi$), C ($M = 0.9$, $\theta = \pi$), D ($M = 0.5$, $\theta = 0$), E ($M = 0.6$, $\theta = 0$), and F ($M = 0.9$, $\theta = 0$) are validated cases investigated in this work.

$$\frac{U_1}{\mathrm{i}\omega}\frac{\partial\varphi(\boldsymbol{x};\boldsymbol{y})}{\partial y_1} = \frac{U_1}{U_p} = \frac{M}{M-1} \tag{25}$$

The series of surface integrals converges when

$$\left|\frac{U_1}{\mathrm{i}\omega}\frac{\partial\varphi(\boldsymbol{x};\boldsymbol{y})}{\partial y_1}\right| < 1$$

which corresponds to $0 < M < 0.5$. Therefore, the computation of the quadrupole term at the upstream observer positions by using the series in Eq. (19) diverges in the case with $M = 0.6$. It is clear that the physics corresponding to the divergence is that the convective velocity is larger than the phase velocity of a perturbation propagating through the convective flow. The convergence of the series in Eq. (19) can be expressed in terms of Mach number and directivity since the phase velocity depends on the Mach number and the directivity. Figure 2 provides a diagram to show the convergence of the series in Eq. (19) at different directivities where $\theta = 0$ and π correspond to the downstream and upstream observers, respectively. The series in Eq. (19) converges when the Mach number is below the dashed line, whereas the proposed model [Eq. (18)] is valid above the dashed line (as is the case at $M = 0.6$ and $M = 0.9$ in Figs. 1b and 3b) as well as below (as is the case at $M = 0.6$, $M = 0.9$, and $M = 0.5$ in Figs. 1a, 3a, and 4a) and on the dashed line ($M = 0.5$ in Fig. 4b). The results show that the proposed model can correctly approximate the volume integral of the quadrupole term and effectively diminish the error associated with the vortices crossing the FW-H integral surface. The proposed model is robust in computing the sound at different directivities and different subsonic Mach numbers.

V. Conclusions

The Ffowcs Williams and Hawkings integrals might generate strong spurious sound when vortical flows pass the integral surfaces. This spurious sound can be diminished by accounting for the quadrupole term in a volume external to the integral surface. In this short Note, a model is derived to evaluate the volume integral in the frequency domain by modeling the Lighthill stress fluxes on the surfaces. The proposed model uses different ways of integration by parts to convert the volume integral into surface integrals, which circumvents the divergence problem in computing sound at the upstream observer positions. It is found that the divergence is due to the convective velocity being larger than the phase velocity of a perturbation propagating through the convective flows. The

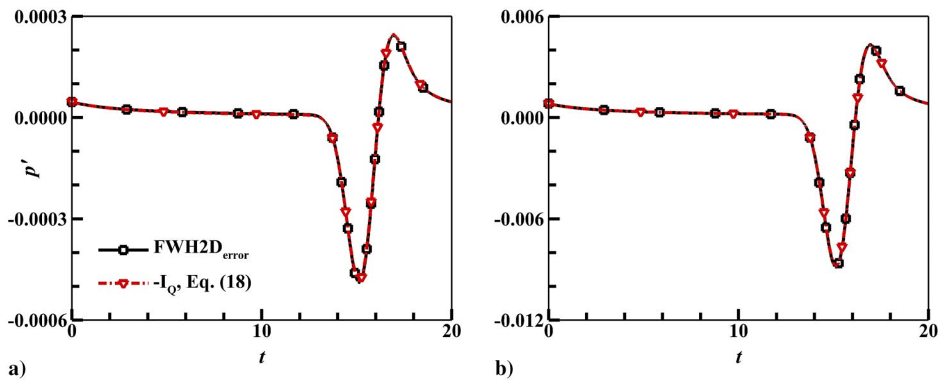

Fig. 3 Comparison of the quadrupole correction I_Q to the errors produced by FWH2D ($I_L + I_T$) at $M = 0.9$ at a) downstream observer ($\theta = 0$) and b) upstream observer ($\theta = \pi$).

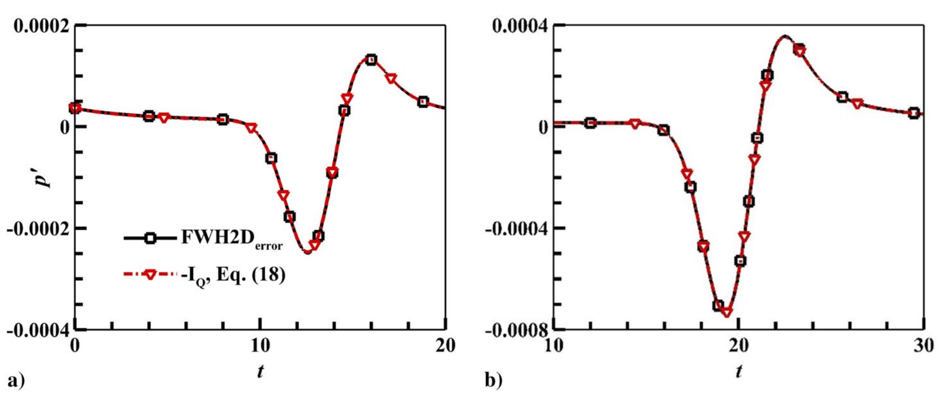

Fig. 4 Comparison of the quadrupole correction I_Q to the errors produced by FWH2D ($I_L + I_T$) at $M = 0.5$ at a) downstream observer ($\theta = 0$) and b) upstream observer ($\theta = \pi$).

results show that the proposed model is valid even for larger convection velocity and smaller phase velocity of perturbations propagating through the convective flow. The frozen flow assumption is employed to avoid calculating the high-order derivatives of the Lighthill stress tensor, and far-field asymptotics are employed to calculate the integrals and derivatives of Green's function, resulting in a computationally efficient single surface integral instead of a series of surface integrals. The proposed model is used to compute the sound generated by a convecting vortex, and the robustness of the proposed model is verified for flows with different subsonic Mach numbers. It should be noted that the proposed model is suitable to compute the far-field sound since the asymptotics of Green's functions are used. The mathematical analysis of the proposed model is provided at separate Mach regions for subsonic flows. The proposed model is expected to be validated by complex flows when different Mach regions coexist.

Acknowledgments

This work is supported by the National Nature Science Foundation of China Basic Science Center Program for "Multiscale Problems in Nonlinear Mechanics" (no. 11988102), the National Natural Science Foundation of China (nos. 11922214, 91752118, and 91952301), and the National Numerical Windtunnel project. The authors would like to acknowledge the support from the Strategic Priority Research Program of the Chinese Academy of Sciences (XDB22040104). The computations are conducted on Tianhe-1 at the National Supercomputer Center in Tianjin.

References

[1] Ffowcs Williams, J. E., and Hawkings, D. L., "Sound Generation by Turbulence and Surfaces in Arbitrary Motion," *Philosophical Transactions of the Royal Society of London, Series A: Mathematical and Physical Sciences*, Vol. 264, No. 1151, 1969, pp. 321–342. https://doi.org/10.1098/rsta.1969.0031

[2] Ikeda, T., Enomoto, S., Yamamoto, K., and Amemiya, K., "Quadrupole Corrections for the Permeable-Surface Ffowcs Williams–Hawkings Equation," *AIAA Journal*, Vol. 55, No. 7, 2017, pp. 2307–2320. https://doi.org/10.2514/1.J055328

[3] Yao, H.-D., Davidson, L., and Eriksson, L.-E., "Noise Radiated by Low-Reynolds Number Flows Past a Hemisphere at Ma = 0.3," *Physics of Fluids*, Vol. 29, No. 7, 2017, Paper 076102. https://doi.org/10.1063/1.4994592

[4] Spalart, P. R., Belyaev, K. V., Shur, M. L., Kh Strelets, M., and Travin, A. K., "On the Differences in Noise Predictions Based on Solid and Permeable Surface Ffowcs Williams–Hawkings Integral Solutions," *International Journal of Aeroacoustics*, Vol. 18, Nos. 6–7, 2019, pp. 621–646. https://doi.org/10.1177/1475472X19878934

[5] Zhong, S., and Zhang, X., "A Sound Extrapolation Method for Aeroacoustics Far-Field Prediction in Presence of Vortical Waves," *Journal of Fluid Mechanics*, Vol. 820, June 2017, pp. 424–450. https://doi.org/10.1017/jfm.2017.219

[6] Mao, Y., and Hu, Z., "Analysis of Spurious Sound due to Vortical Flow Through Permeable Surfaces," *Aerospace Science and Technology*, Vol. 96, Jan. 2020, Paper 105544. https://doi.org/10.1016/j.ast.2019.105544

[7] Wang, M., Lele, S. K., and Moin, P., "Computation of Quadrupole Noise Using Acoustic Analogy," *AIAA Journal*, Vol. 34, No. 11, 1996, pp. 2247–2254. https://doi.org/10.2514/3.13387

[8] Nitzkorski, Z., and Mahesh, K., "A Dynamic End Cap Technique for Sound Computation Using the Ffowcs Williams and Hawkings Equations," *Physics of Fluids*, Vol. 26, No. 11, 2014, Paper 115101. https://doi.org/10.1063/1.4900876

[9] Rahier, G., Huet, M., and Prieur, J., "Additional Terms for the Use of Ffowcs Williams and Hawkings Surface Integrals in Turbulent Flows," *Computers and Fluids*, Vol. 120, Oct. 2015, pp. 158–172. https://doi.org/10.1016/j.compfluid.2015.07.014

[10] Ikeda, T., Yamamoto, K., and Amemiya, K., "The Frequency-Domain Formulations of the Quadrupole Correction for the Ffowcs Williams-Hawkings Integration," *Aeroacoustics Conferences*, AIAA Paper 2016-2794, 2016. https://doi.org/10.2514/6.2016-2794

[11] Lockard, D., and Casper, J., "Permeable Surface Corrections for Ffowcs Williams and Hawkings Integrals," *11th AIAA/CEAS Aeroacoustics Conference*, AIAA Paper 2005-2995, 2005.

[12] Lockard, D. P., "An Efficient, Two-Dimensional Implementation of the Ffowcs Williams and Hawkings Equation," *Journal of Sound and Vibration*, Vol. 229, No. 4, 2000, pp. 897–911. https://doi.org/10.1006/jsvi.1999.2522

[13] Guo, Y., "Application of the Ffowcs Williams/Hawkings Equation to Two-Dimensional Problems," *Journal of Fluid Mechanics*, Vol. 403, Jan. 2000, pp. 201–221. https://doi.org/10.1017/S0022112099006989

[14] Zhou, Z., Wang, H., and Wang, S., "Simplified Permeable Surface Correction for Frequency-Domain Ffowcs Williams and Hawkings Integrals," *Theoretical and Applied Mechanics Letters*, Vol. 11, June 2021, Paper 100259. https://doi.org/10.1016/j.taml.2021.100259

D. Papamoschou
Associate Editor